

## **EFFECTS OF BIOMASS GROWTH ON PRESSURE DROP IN SUBMERGED AERATED BIOREACTORS**

**Dr.Dheyaa Wajid Abbood  
Al-Mustansiriyah University  
College of Engineering**

### **Abstract**

A semi-empirical model was developed to predict biomass-affected porosity, specific surface area and pressure drop as a function of the biomass concentration in two selected Submerged Aerated bioreactors (SABRs). Under similar conditions two bench-scale SABRs (1m long and 100mm diameter) were operated to treat an industrial wastewater, the first packed with porcelinaite rocks and the other with polystyrene grains at hydraulic loading rates of ( 0.1–3.2 m/h) and with BOD<sub>5</sub> concentration of (110- 436 mg/L) .

Typical constant that can be used to estimate pressure drop for some of the most common design of SABRs were correlated. The proposed equations in porosity and specific surface area caused by biomass accumulation in SABR bed are based on macroscopic estimates of average biomass concentrations. In comparison to biofilm-based models, the macroscopic models are relatively simple to implement and are computationally more efficient.

The effects of biomass accumulation and distribution on pressure losses and removal efficiency of biological load in SABRs were experimentally studied.

Localized biomass accumulation in the SABR beds is the key factor increasing the pressure drop, which was caused by local bed clogging due to biomass growth. The highest pressure drops in the beds (porcelinaite rocks: 2,150 N/m<sup>3</sup> and polystyrene grains: 1115 N/m<sup>3</sup>) occurred where there were high biomass levels. The pressure drop varied nonlinearly with the amount of accumulated biomass and the amount of oxygen consumed.

Porcelinaite rocks caused greater pressure drops, on average 2 times higher than the polystyrene grains. Compaction, as a consequence of biomass growth and porcelinaite rocks degradation increased the pressure drop in the porcelinaite rocks bed. A comparison of the experimental and the predicted pressure drops showed that the model provided good estimates of biomass-affected porosity and pressure drop in the SABRs packed with spherical grains with even biomass distribution.

**Keywords: pressure drop, aerated submerged bioreactor, biomass growth, porcelinaite rocks**

## تأثير نمو الكتلة الحيوية على هبوط الضغط في مفاعل حيوي غاطس مهوى

د. ضياء واجد عبود

الجامعة المستنصرية

كلية الهندسة

**المستخلص:**

تم تطوير نموذج شبه تجريبي للتنبؤ بتأثير الكتلة الحيوية على المسامية، المساحة السطحية النوعية وهبوط الضغط كدالة تركيز الكتلة الحيوية في مفاعلين حيويين غاطسين مهواة.

شُغل المفاعلين تحت نفس الظروف بمقياس مختبري بحجم (1)  $\square \square$  100 ملم قطر للمفاعل وباستخدام مياه صناعية عادمة من معامل النسيج في بغداد. تم حشو المفاعل الاول بصخور البورسيلينات والآخر بحبيبات البوليستايرين بمعدل حمل هيدروليكي (0.1 - 3.2 م/ساعة) وتركيز للطلب الاوكسجين الحيوي الكيماوي BOD5 (110 - 436 ملغم/لتر).

تم تعيير المعاملات الثابتة المستخدمة لتقدير هبوط الضغط في تصاميم المفاعلات الحيوية الغاطسة المهواة. اعتمد في تخمين المعادلات المقترحة للمسامية والمساحة السطحية النوعية المتأثرة بتراكم الكتلة الحيوية في المفاعلات الحيوية الغاطسة على النماذج المايكروية لمتوسط تراكيز الكتلا لحيوية. بالاعتماد على النماذج الكتلة الحيوية، وُجد ان النماذج المايكروية بسيطة نسبياً في الاستخدام وحسابياً غير مكلفة. درست تأثير تراكم الكتلة الحيوية وتوزيعها على هبوط الضغط وكفاءة الازالة مع الحمل الحيوي في المفاعلات الحيوية الغاطسة المهواة تجريبياً. ان تراكم الكتلة الحيوية في الاوساط المسامية للمفاعلات الحيوية هي عامل اساسي لزيادة الضغط بسبب انسداد هذه الاوساط بفعل النمو الكتلي الحيوي.

كان اعلى هبوط ضغط في وسط صخور البورسيلينات 2150 نيوتن/م<sup>3</sup> وفي وسط حبيبات البوليستايرين 1115 نيوتن/م<sup>3</sup> عند مستويات عليا للكتلة الحيوية. وجد ان هبوط الضغط يتغير لاختطياً مع كمية الكتلة الحيوية المتراكمة ومع كمية الاوكسجين المستهلك.

اظهرت النتائج ان صخور البورسيلينات سببت هبوط ضغط عالي بلغ مرتان من هبوط الضغط المسبب بواسطة حبيبات البوليستايرين. ان تأثير الرص كمتسلسة لنمو الكتلة الحيوية ساهم ي ازدياد وهبوط الضغط في صخور البورسيلينات. بينت نتائج مقارنة القياسات التجريبية والمقدرة لهبوط الضغط ان تخمين النموذج النظري جيد لتأثير الكتلة الحيوية على المسامية والضغط.

### **Introduction**

Submerged aerated biological filter SBAF is economically efficient technology for industrial wastewater, and also used for the biological treatment of moist, dilute airstreams contaminated with odorous, toxic, and volatile organic compounds (Leson and Winer 1991). The pollutants are degraded by a microbial community that develops under optimized conditions of humidity, temperature, and pH within the bed.

In a biofilter, the synthesis of microbial mass (biomass) by the mineralization of biodegradable pollutants leads to biomass growth and accumulation over time, which has been related to an increase in flow resistance in the bed [e.g., Kinney et al. (1996) and Mohseni et al. (1998)]. Biomass accumulation, which is greater at the inlet sections of biofilters (Corsi and Seed 1995), leads to a change in bed characteristics, such as the reduction of the interparticle void space and the compaction of natural packing materials, which cause channeling and increased pressure drops. This translates into higher operating and maintenance costs that become significant for long-term biofilter operation. A better understanding of the growth of biomass in biofilters and the effects on flow may lead to improved designs with reduced energy requirements, lower operating and maintenance costs and increased removal capacities. This knowledge will also help to identify sources of operational problems and to formulate measures for improving the biofiltration process.

Three distinct approaches to model microbial growth and accumulation processes in porous media include the continuous biofilm, discrete micro colony, and macroscopic approaches (Baveye and Valocchi, 1989). The biofilm approach assumes continuous and uniform biomass growth on the exposed surface of each particle in a porous medium. Taylor and Jaffe (1990a, b, c) and Taylor et al. (1990) used this assumption to derive analytical expressions to model changes in porous media properties due to biological growth. However, as pointed out by Baveye and Valocchi (1989), Taylor and Jaffe's (1990) experimental study presented no supporting evidence to verify the actual growth patterns and film thicknesses of the attached biomass. Cunningham et al. (1991) also proposed expressions to model the influence of biofilm accumulation on hydrodynamics in porous media. However, use of these expressions is limited to cubically packed spherical media with particles of uniform diameter. Alternatively, Vandevivere and Baveye (1992a, b) support the microcolony model for biomass growth since they observed discrete microbial colonies in a biologically active saturated sand column. Microbial growth inside the column was sparse and heterogeneous. In reality, growth patterns in porous media are more likely a combination of the two models, where microbes initially grow in discrete colonies and gradually expand to form continuous biofilms (Rittmann, 1993). Therefore, the macroscopic approach, the third alternative which considers only spatially averaged biomass concentrations, is a more realistic option for describing

biomass in porous media. This option offers more adaptability because it does not suppose any specific growth pattern. It is also the approach most commonly reported in the literature (Corapcioglu and Haridas, 1984). Moreover, in most microbially mediated transport studies involving porous media, experimental data for microbes are reported only as average biomass concentrations (Taylor and Jaffe, 1990). The biomass layers appeared very gel-like and had a high water content and high concentrations of extracellular polymeric substances (EPSs) (Morgan-Sagastume 1999).

The pressure drop through a biofilter bed typically ranges from 20 to 100 Pa/m and can even go up to 1000 Pa/m, and typical superficial air velocities may vary from 5 to 500 m<sup>3</sup>/m<sup>2</sup> h (Devanny et al. 1999). Systems with adequate moisture control and a porous medium containing bulking agents will typically achieve pressure losses <900–1,700 Pa/m (Leson and Smith 1997). Various researches have reported flow pressure losses in biofilters in relation to the bed particle size (Van Langenhove et al. 1986; Corsi and Seed 1995); nature and composition of the filter medium (Mohseni et al. 1998); bed content (Sabo et al. 1993); and time of operation. Some studies have related increases in pressure drop to biofilm growth and clogging by biomass (Hodge et al. 1992). For example, Liu et al. (1994), working with granular activated carbon columns for toluene removal, measured increased pressure drops of up to 12 kPa/m due to biomass accumulation and airflow channeling. In general, the increase in pressure drop as a result of biomass development in biofilters can be explained by a decrease in the bed interparticle void space or the effective porosity or both and by the microbial degradation of the support matrix, as in the case of natural media, which result in decreased specific permeability. Although the effect of biomass accumulation on pressure drop has been studied in biotrickling filters treating a gaseous stream (Okkerse et al. 1999),

there has not been detailed, quantitative research on this phenomenon in biofilters.

***The aim of this paper*** is to:-

- Model changes in porosity and specific surface area caused by biomass

accumulation in porous media. the macroscopic approach is adopted and used

attached biomass concentration as the model variable to describe variations in porous media properties.

- Study the influence of biomass accumulation on pressure drop in submerged biological aerated reactor that treat organic compounds.
- Model pressure losses caused by biomass growth in SABR using semi empirical models.
- Evaluate the interparticle porosity and pressure drop changes due to biomass accumulation in a SABR.

## **Experimental Approach**

### **1-Experimental Setup**

A biofiltration system consisting of two identical laboratory scale SABRs were used to treat industrial wastewater from woolltextile industry in Baghdad Plate(1). For each biofilter, wastewater was passed through stainless steel column (100mm diameter and 1m height), packed and regulate its temperature in the SABR in the range of 24 – 26°C.

A small and controlled airflow from the inlet air-stream was compressed and passed through a stainless-steel vessel which then was fed to the top of the SABR. The biological oxygen demand BOD<sub>5</sub>, chemical oxygen demand COD, and total solids TS were monitored every run from wastewater samples taken at the inlet and the outlet of each SABR. Manometer was used to measure differential pressure along segments of the beds, between axial ports located at the top, middle, and bottom of each section. The minimum detectable differential pressure reading of the manometer was 2.5 Pa (0.25mm. water). The amount of biomass developed on the packing materials was assessed in both biofilters from bed composite samples taken from the top and bottom of each bioreactor.

Sampling was performed on a periodic basis, every 2–3 weeks. In total, eight samplings were performed during this experiment. After sampling, the packing material within each biofilter was remixed to ensure a uniform biomass distribution at the beginning of each period of operation.

### **2-Packing Media**

One SABR was packed with sieved porcelinite rock (1228kg dry /m<sup>3</sup> bioreactor ) with a size range of (2.5-4mm). These types of porcelinite rock were used successfully in previous biofiltration experiments. The porcelanite rocks samples used

in this study were supplied from the General Company for Geological Survey and Mineralogy-Ministry of Industry and Minerals (GCGSM). The porcelanite rocks were prepared for the present work by grinding and sieving to obtain a grain size range (0.65-0.8) mm (passing 0.8mm standard sieve and retained on 0.65mm sieve) and then washed with distilled water and dried in an oven at 105°C for 4hr. The porcelanite rock has been analyzed by the method used in (GCGSM); the result is shown in **Table (1)**.

Chemically, diatomite consists primarily of silicon dioxide ( $\text{SiO}_2$ ), and is essentially inert. It is attacked by strong alkalizes and by hydrofluoric acid, but it is practically unaffected by other acids. Because of the intricate structure of the diatom skeletons that form diatomite, the silicon dioxide has a very different physical structure from other forms in which it occurs. The chemically combined water content varies from 2 to 10%. Impurities are other aquatic fossils (sponge residues, radiolar, and silica-flagellate), sand clay, volcanic ash, calcium carbonate, magnesium carbonate, soluble salts, and organic matter. The types and amount of impurities are highly variable and depend upon the conditions of sedimentation at the time of diatom deposition. The **Table (1)** indicates that the silica content of the Iraqi deposits are 70.4% which is around 20% lower than that of American and Spain deposits with higher content of CaO and L.O.I.

With its high quality the Iraqi porcelanite is highly competitive in spite of the presence of iron when compared with the USA and Algerian diatomite **Table (2)**. Iron content is one of the important factors for the determination of mineral quality, as iron can form complexes when diatomite is used in chemical and biochemical processes.

**Table (3)** indicates some physical analysis for Iraqi rocks.

The color of pure diatomite is white, or near white, but impurities such as carbonaceous matter, clay, iron oxide, volcanic ash, may darken it. The refractive index ranges from 1.41 to 1.48. Diatomite is isotropic. The true specific gravity of diatomite is 2.1-2.2; the fusion point average about 1590°C for pure material.

The other SABR was packed with polystyrene (32 kg dry /m<sup>3</sup> bioreactor; with diameters of (4-6mm), Eight liters of packing material were randomly packed in each SABRs

The polystyrene have been successfully used in *SABRs*, and they were used in this experiment because they provide interference-free biomass quantification and have a defined spherical shape and size for pressure drop modeling.

### 3- Hydrodynamic modeling

In packed beds with biofilm growth, if the biofilm thickness remains small compared to the effective pore space, accumulation of biofilm will not significantly affect the distribution of fluid velocities within a porous medium (Cunningham et al . 1990). However, if the biofilm occupies a significant fraction of the effective pore space, a decrease in porosity will occur as shown in **Figure(1)**. It is possible to reduce the number of variables appearing and to make this compact results ((equation or chart) applicable to all similar situation. Investigations consider the bed of porous media as composed of a number of capillary pores, passing in parallel, straight through the depth of the bed .In this case the head loss in high flow velocity (turbulent flow) depend upon capillary water velocity ( $V_c$ ), dynamic viscosity ( $\mu$ ), density ( $\rho$ ). Using dimensional analysis (Buckingham  $\Pi$  theorem), general form of the empirical relationship can be constructed as follow: -

$$(1) \frac{\Delta H}{L} = \Psi(\text{Re}) \frac{1}{d_c} \frac{V_c^2}{2g}$$

$$V_c = \frac{Q}{nA_b} = \frac{V \zeta}{n} \quad (2)$$

$$\text{And } n = \frac{\nabla_v}{\nabla} \quad (3)$$

Where  $L$ : length of capillary (L),  $\mu$  : dynamic viscosity (M/L.T),  $\rho$  : density (M/L<sup>3</sup>),  $g$ : standard acceleration of gravity,(9.81m/s<sup>2</sup>),  $d_c$ : inside diameter of capillary(L) and  $V_c$ : velocity of fluid in capillary (L/T).  $n$  : bulk porosity of bed of porous media (L<sup>3</sup>/L<sup>3</sup>),  $\nabla_v$  : volume of the voids (L<sup>3</sup>),  $\nabla$  : total volume of the bed (L<sup>3</sup>),  $\zeta$  : tortuosity (L/L).

$\Psi(Re)$  is function to Reynolds number ( $Re$ ) which is one of the most important dimensionless parameters in high flow velocity in porous media and its size determines the nature of flow. Turbulent flow in pipe, friction factor can be evaluated from (Blasius formula): -

$$f = \frac{0.316}{Re^{0.25}} \quad (4)$$

Similar to (Blasius formula) the hydraulic resistance factor ( $C_f$ ) in porous media can be simulated as function to friction factor and as the form: -

$$C_f = \frac{C'_f}{Re^{.25}} \quad (5)$$

$$\text{And } Re_{pore} = \frac{4\zeta \rho V}{\mu (1-n) S} \quad (6)$$

Where  $C'_f$ : constant depends upon porosity( $n$ ), uniform factor ( $\Phi$ ), and grain shape of media. Because of extreme complexity of grains shape of the media and its arrangement (spacing between the grains) most of the advance in understanding the basic relation have been developed around experiments on grains shape or initial specific surface area per volume of clean substratum ( $m^2/m^3$ ),  $S_o$  which is defined as:

$$(7) \frac{3(1-n_o)}{\phi.R} S_o =$$

The average shape or sphericity factor for the porcelinite spherical grain size was assumed to be 0.85, based on values of (0.75-0.95) for nearly spherical of various sand types (Perry and Green 1988). The expression proposed for calculating biomass-affected porosity  $n_b$  in a bed packed with spheres, where biomass grows uniformly on the sphere surfaces (**Figure (1)**):

$$n_b = n_o - n_{fv} \quad (8)$$

$$\forall_{mr} = \frac{1 - n_b}{1 - n_o} \quad (9)$$



$$\forall_{mr} = \left(1 - \frac{L_b}{R}\right)^3 - \frac{N}{4} \left(\frac{L_b}{R}\right)^2 \left(2\frac{L_b}{R} + 3\right) \quad (10)$$

where :  $\phi$  = sphericity factor for the packing solids;  $n_0$  = initial porosity of the bed without biofilm  $L^3/L^3$ ;  $n_b$  = the biomass-affected porosity;  $n_{fv}$  = Volume fraction of the biomass ( $L^3$  biomass/  $L^3$  total);  $L_b$  = biofilm thickness ( L ),  $\forall_{mr}$  = accumulative volume ratio of the packing medium ( $L^3$  biomass/  $L^3$  bed);  $R$  = radius of a sphere equivalent to the packing medium L ; and  $N$  = number of packing spheres in contact with a single sphere or coordination number. Eq. (10) was deduced for spheres in contact, upon which biofilm grow uniformly, leaving the contact points uncovered. The coordination number  $N$  that accounts for the number of contact points among the spheres can be estimated from an expression (Dullien 1992) correlating porosity  $n$

$$N = 13.84 \pm \sqrt{(191.4 - 231.9 n)} \quad (11)$$

The thickness  $L_b$  of the biofilm growing on the packing material can be calculated as follows:

$$L_b = \frac{X}{\rho_b} \quad (12)$$

where  $X$  = superficial biomass concentration (g biomass/ $m^2$  surface area); and  $\rho_b$  = biofilm density (g biomass/ $m^3$  biomass) (M biomass/ $L^3$  biomass)..

The fraction of volume occupied by the solid-phase biomass can be estimated as :-

$$\forall_{mr} = \frac{\rho_s X_m}{\rho_b} \quad (13)$$

where  $X_m$  is the mass (dry weight) of microbial cells per unit mass of solids (M of microbial mass /M of bed). Based on volume balances, a simple macroscopic equation Volume fraction of the biomass  $n_{fv}$  can be expressed as :-

$$n_{fv} = \frac{1}{3} \phi R (\forall_{mr} - 1) S_o \quad (14)$$

Volume fraction of the biomass  $n_{fv}$  can be approximate as function to specific surface area, and biofilm thickness ( Taylor et al. (1990))

$$n_{fv} = L_b S_o$$

(15)

Using this porosity relationship, equations ( 7) and (8) are modified to estimate biomass-affected specific surface area ( $S_b$ ) values

$$S_b = \frac{3(1 - n_b)}{\phi \cdot R \left(1 + \frac{L_b}{R}\right)}$$

(16)

for computing specific surface area reduction , biomass-affected specific surface area ratio related to porosity ratio can be expressed as

$$\frac{S_o}{S_b} = \left(\frac{n_b}{n_o}\right)^{0.5}$$

(17)

Values of specific surface area are typically unimportant except in the biofilm approach where they are required to compute film thicknesses. Although the macroscopic approach does not explicitly consider biofilms, it is possible to estimate apparent biofilm thicknesses through macroscopic model-based equations (17) . These film thicknesses can be useful in modeling diffusion limitations across attached biomass (Rittmann and McCarty, 1981). Analytical models for predicting changes in porosity and specific surface area due to microbial growth in porous media are developed from a macroscopic approach. Variations in SABR properties are computed from macroscopic averaged attached biomass concentrations. The macroscopic models developed in this work are easy to implement and computationally more efficient than the biofilm models. The macroscopic expressions can be explicitly used to estimate biomass-affected porosity and specific surface area, at any attached biomass concentration. Since the biofilm models of Taylor et al. (1990) are implicit functions of attached biomass thickness, these porous media properties cannot be estimated explicitly.

A comparison of experimental results and estimated results based on our macroscopic biofilm models is presented for predictions of relative changes in

porosity (**Figure(1)**). Simulation experiments started with clean media( without biomass) which the head loss in SABR can be formulated as follow :-

$$\frac{\Delta H}{L} = C'_f \left(\frac{\mu}{\rho}\right)^{0.25} \left\{\frac{(1-n)^{1.25}}{n^3}\right\} S^{1.25} \zeta^{1.75} V^{1.75}$$

(18)

Analyses of experimental results show that the effect of biomass on head loss per bed depth in SABR s can be evaluated by the modified equation

$$\frac{\Delta H}{L} = C'_f \left(\frac{\mu}{\rho}\right)^{0.25} \left\{\frac{(1-n)^{1.25}}{n^3}\right\} S^{1.25} \zeta^{1.75} V^{1.75} \forall_{mr}$$

(19)

For modeling the effect of biomass on pressure drop in SABR s using the above equations, the following assumptions are made:

- the packing material is composed of homogenous particles.
- biomass grows uniformly on the surface of spheres or of other particles with an equivalent diameter of a sphere of the same surface area.
- the spheres remain in contact during biomass accumulation, which assumes biofilm growth on the whole surface of the spheres; and
- biomass has a constant density within the biofilm, which can be assumed at a macro scale, even if at a micro scale there is strong evidence of high biofilm heterogeneity (Bishop 1997).

### **Experimental results**

At the highest flow rates, the increase in pressure drop and the increase of the degree of curvature of the lines suggest that kinetic energy losses became important. The kinetic energy losses as a function of the flow rate squared and the reduction of the bed porosity **Figure (1)**.The general approach in modeling the effects of biomass accumulation on pressure drop in the polysteren biofilter involved estimating porosity changes and pressure drops in the SABR based on the experimental concentrations of biomass (g biolayer/g dry substratum) and on waste water flow rates (**Figure(2)**).The comparsoin between the experimental results of head loss of water per bed depth and proposed equation (19) gives acceptable approximation (**Figure(3)**).

Localized high biomass content in the SABR beds was the key factor affecting increased pressure drop in both SABRs caused by local clogging or local void space

reduction or both. The effect of accumulated an incremental amount of biomass for different times and on pressure drop were correlated with a reasonable approximation in **Figures (4) to (6)**. The pressure drop in the porcelinite rock biofilter was twice that in the polystyrene SABR. This difference was believed to be due to greater biomass growth in the porcelinite rock bed (polystyrene polystyrene: 0.4–3.2 g biolayer/g dry substratum; porcelinite rock: 0.5–19 g biolayer/g dry substratum) and a different pore structure

Biofilm thickness values were first estimated from the biomass concentrations (g biolayer/g dry substratum) in the bed. For this, the biomass concentrations were converted from grams of biolayer per grams of dry substratum to grams of biomass per square meters of substratum surface, using the dry substratum bulk density and an estimated initial superficial area of the packed substratum.

Differences between predicted and experimental pressure drops in the polystyrene SABR and porcelinite rock SABR before remixing are due to uneven biomass distribution at high biomass concentrations, which is not thoroughly characterized by averaging biomass concentration over a specific bed volume.

The profiles of detached biolayer for both the polystyrene SABR and porcelinite rock SABR show that most of the biomass accumulated in the first half of the bed and the biomass concentrations in the porcelinite rock bed were roughly 180% to 210% higher than in the polystyrene SABR. The biomass accumulation on the porcelinite rocks bed played the main role in controlling the pressure drop increase, compared to compaction.

High concentrations at the top of both the polystyrene SABR and porcelinite rock SABR on day 76 in the porcelinite rock SABR correspond to the observed formation of biomass layers (0.3–0.4 cm) on the top of these sections, which caused the highest pressure drops during the experimental period

Biomass water content in these layers was as high as 29–61 g water/g TS in the polystyrene biofilter, compared to 13–15g water/g TS in the rest of the bed, and in the porcelinite biofilter as high as 97–122g

### **Summary Concentrations**

- A semi empirical model was developed to predict pressure drop from biomass concentrations in a SABR bed by modification the pressure drop in porous media equation as a function of bed porosity and biomass affected porosity.

The model is a good estimate for predicting biomass-affected porosity in beds packed with spherical particles where biomass grows evenly distributed, and it successfully predicts pressure drop for the case of even biomass growth on spherical particles as follow:-

$$\frac{\Delta H}{L} = C'_f \left(\frac{\mu}{\rho}\right)^{0.25} \left\{\frac{(1-n)^{1.25}}{n^3}\right\} S^{1.25} \zeta^{1.75} V^{1.75} \nabla_{mr}$$

- The optimal utilization of a SABR bed strongly depends on biomass distribution within the bioreactor and not just on the amount of biomass growing on the packing material. The highest pressure drops in the beds were caused by layers of biomass which increased the biomass specific volume and significantly decreased the bed porosity at the top levels of the biofilters.
- porcelinite rocks SABR caused greater pressure drops, on average 2 times higher than the polystyrene SABR. Compaction, as a consequence of biomass growth degradation, together with water content, increased the pressure drop in the porcelinite rocks bed.
- The proposed models can be used as simple tools for estimating changes SABR properties during biological process.

### **References**

1. Auria, R., Morales, M., Villegas, E., and Revah, S. (1993). "Influence of mold growth on the pressure drop in aerated solid state fermentors." *Biotechnology and Bioengineering*, 41(11), 1007–1013.
2. Bailey, J. E., and Ollis, D. F. (1986). *Biochemical engineering fundamentals*, 2nd Ed., McGraw-Hill, New York.
3. Baveye, P. and V. A. Valocchi. 1989. An evaluation of mathematical models of the transport of biologically reacting solutes in saturated soils and aquifers. *Water Resources Research*. v. 25, pp. 1413-1421.
4. Bishop, P. L. (1997). "Biofilm structure and kinetics." *Water Sci. and Technol.*, 36(1), 287–294.
5. Corapcioglu, M. Y. and A. Haridas. 1984. Transport and fate of microorganisms in porous media: A theoretical investigation. *Journal of Hydrology*. v. 72, pp. 149-169.
6. Corsi, R. L., and Seed, L. (1995). "Biofiltration of BTEX: Media, sub-strate, and loadings effects." *Envir. Progress*, 14(3), 151–158.

7. Cunningham, A. B., Bouwer, E. J., and Characklis, W. G. (1990). "Bio-films in porous media." *Biofilms*, W. G. Characklis and K. C. Marshall, eds., Wiley, New York, 697–732.
8. Cunningham, A. B., W. G. Characklis, F. Abedeen, and D. Crawford. 1991. Influence of biofilm accumulation on porous media hydrodynamics. *Environmental Science and Technology*. v. 25, pp. 1305-1311.
9. Devinny, J. S., Deshusses, M. A., and Webster, T. S. (1999). *Biofiltration for air pollution control*, Lewis, Boca Raton, Fla. Dullien, F. A. L. (1992). *Porous media: Fluid transport and pore structure*, 2nd Ed., Academic, San Diego.
10. Dullien, F.A.L. 1979. *Porous Media fluid Transport and Pore Structure*. Academic Press, San Diego, CA. 941
11. Kinney, K. A., Chang, D. P. Y., Schroeder, E. D., and Scow, K. M. (1996). "Performance of a directionally-switching biofilter treating toluene contaminated air." *Proc., 89th Annu. Meeting and Exhibition of the Air and Waste Mgmt. Assn.*
12. Hodge, D. S., Medina, V. F., Wang, Y., and Devinny, J. S. (1992). "Bio-filtration: Application for VOC emission control." *Proc., 47th Purdue Industrial Waste Conf., Lewis, Boca Raton, Fla., 609–619.*
13. Liu, P. K. T., Gregg, R. L., Sabol, H. K., and Barkley, N. (1994). "Engineered biofilter for removing organic contaminants in air." *Air & Waste*, 44(March), 299–303.
14. Lozada, D. S., P. Vandevivere, P. Baveye, and S. Zinder. 1994. Decrease of the hydraulic conductivity of sand columns by *Methanosarcina harken*. *World Journal of Microbiology and Biotechnology*. v. 10, pp. 325-333.
15. Mohseni, M., Allen, D. G., and Nichols, K. M. (1998). "Biofiltration of a-pinene and its application to the treatment of pulp and paper air emissions." *TAPPI J.*, 81(8), 205–211.
16. Morgan-Sagastume, F. (1999). "Effects of biomass growth on pressure drop in biofilters." MASC thesis, Grad. Dept. of Chemical Engrg. And Appl. Chem., University of Toronto, Toronto.
17. Okkerse, W. J. H., Ottengraf, S. P. P., Ozinga-Kuipers, B., and Okkerse, M. (1999). "Biomass accumulation and clogging in biotrickling filters for waste

- gas treatment. Evaluation of a dynamic model using di-chloromethane as a model pollutant.” *Biotechnology and Bioengineering*, 63(4), 418–430.
18. Perry, R. H., and Green, D. (1988). *Perry’s chemical engineers’ hand-book*, 6th Ed., McGraw-Hill International.
  19. Rittmann, B. E. and P. L. McCarty. 1981. Substrate flux into biofilm of any thickness. *ASCE Journal of Environmental Engineering Division*. v. 101, pp. 831-849.
  20. Rittmann, B. E. 1993. The significance of biofilms in porous media. *Water Resources Research*. v. 29, pp. 2195-2202.
  21. Sabo, F., Motz, U., and Fischer, K. (1993). “Development and testing of high-efficiency biofilters.” *Proc., 86th Annu. Meeting and Exhibition of the Air and Waste Mgmt. Assn.*
  22. *Standards methods for the examination of water and wastewater*. (1992). 18th Ed., American Public Health Association, Washington, D.C.
  23. Taylor, S. W. and P. R. Jaffe. 1990a. Biofilm growth and the related changes in the physical properties of a porous medium. I. Experimental investigation. *Water Resources Research*. v. 26, pp. 2153-2159.
  24. Taylor, S. W., P.C.D. Milly, and P. R. Jaffe. 1990. Biofilm growth and the related changes in the physical properties of a porous medium. 2. Permeability. *Water Resources Research*. v. 26, pp. 2161-2169.
  25. Taylor, S. W. and P. R. Jaffe. 1990b. Biofilm growth and the related changes in the physical properties of a porous medium. 3. Dispersivity and model verification. *Water Resources Research*. v. 26, pp. 2171-2180.
  26. Taylor, S. W. and P. R. Jaffe. 1990c. Substrate and biomass transport in a porous medium. *Water Resources Research*. v. 26, pp. 2181-2194.
  27. Vandevivere, P. and P. Baveye. 1992a. Saturated hydraulic conductivity reduction caused by aerobic bacteria in sand columns. *Soil Science Society of America Journal*. v. 56, pp. 1-13.
  28. Vandevivere, P. and P. Baveye. 1992b. Relationship between transport of bacteria and their clogging efficiency in sand columns. *Applied Environmental Microbiology*. v. 58, pp. 2523-2530.

29. Van Langenhove, Wuyts, H. E., and Schamp, N. (1986). "Elimination of hydrogen sulphide from odorous air by a wood bark biofilter." *Water Res.*, 20(12), 1471–1476.

Table (1): Chemical Analysis For Porcelanite  
Local Sample Used In This Study.

<b>Constituent</b>	<b>(%)</b>
Silica (SiO <sub>2</sub> )	68.40
Alumina(Al <sub>2</sub> O <sub>3</sub> )	1.56
Iron oxide (Fe <sub>2</sub> O <sub>3</sub> )	0.63
Titanium oxide (TiO <sub>2</sub> )	0.11
Phosphate (P <sub>2</sub> O <sub>5</sub> )	1.48
Lime (CaO)	9.42
Magnesia (MgO)	5.39
Sodium (Na <sub>2</sub> O)	0.64
Potassium (K <sub>2</sub> O)	0.36
Ignition Loss (L.O.I.)	11.15
Total	99.14



Table (2): Typical Chemical Analysis Of Diatomite In  
Some Different Countries And Iraqi Rocks.

Constituent %	LompocU.S.A.	Japan	Spain	Kenya	Algeria	Iraq
Silica (SiO <sub>2</sub> )	89.72	86	88.6	84.5	75.93	70.4
Alumina(Al <sub>2</sub> O <sub>3</sub> )	3.72	5.8	0.62	3.06	0.98	1.75
Iron oxide (Fe <sub>2</sub> O <sub>3</sub> )	1.09	1.6	0.2	1.86	3.3	0.79
Titanium oxide (TiO <sub>2</sub> )	0.1	0.22	0.05	0.17	0.125	0.1
Phosphate (P <sub>2</sub> O <sub>5</sub> )	0.1	0.03	0.00	0.04	13.74	1.98
Lime (CaO)	0.3	0.7	3	1.8	1.87	10.75
Magnesia (MgO)	0.55	0.29	0.81	0.39	2.32	2.1
Sodium (Na <sub>2</sub> O)	0.31	0.48	0.5	1.19	0.7	0.59
Potassium (K <sub>2</sub> O)	0.41	0.53	0.39	0.91	n.a.	0.14
Ignition Loss (L.O.I.)	3.7	4.4	5.2	6.08	5.02	10.42
Total	99.98	100.05	99.37	100	99.08	99.02

n.a.: not analyzed

Table (3) Physical Analysis For Iraqi Rocks.

Sample No.	Density (kg/m <sup>3</sup> )	Porosity (%)	Specific gravity
1	1221	39.302	2.026
2	1228	45.613	2.217
3	1609	25.407	2.148
4	1396	32.706	2.067
5	1403	41.206	2.381



**Plate(1)**

**Plate (1): The Pilot System**

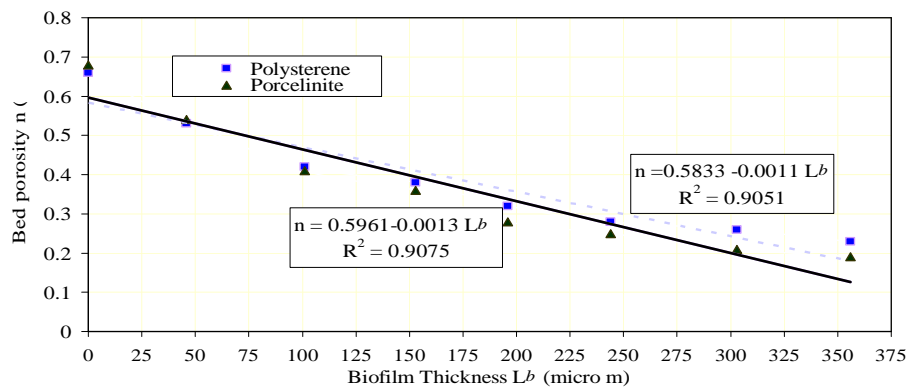


**Figure (1) The Effect Of Biofilm Thickness On Bed Porosity For Different Bed Materials**

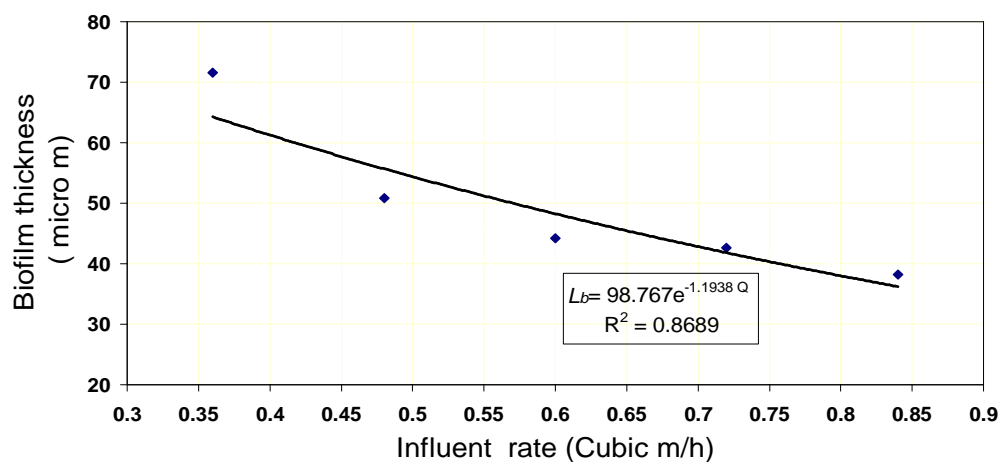


**Figure (2) The Effect Of Influent Rate In Generated Biofilm Thickness On Porcelinaite Surfaces**

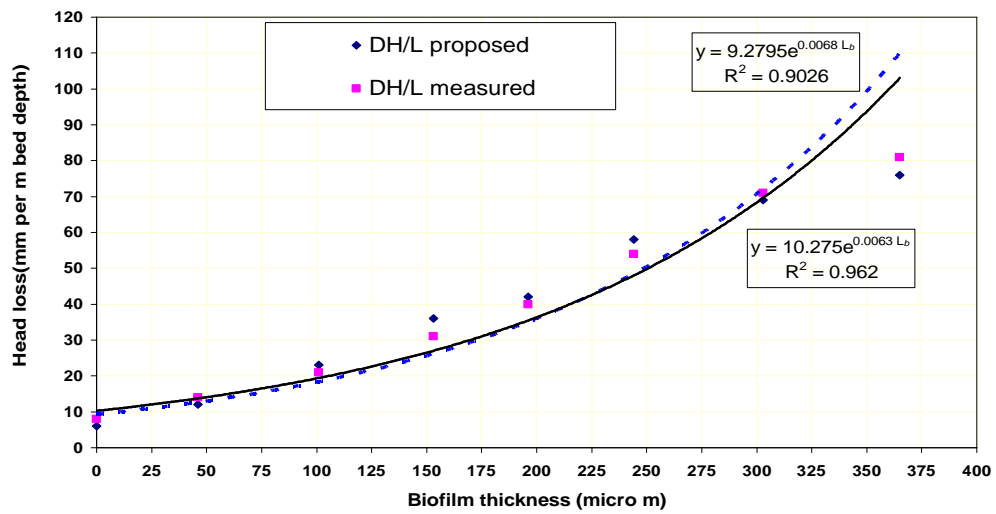


Figure (3) The Comparison Between Proposed And Measured

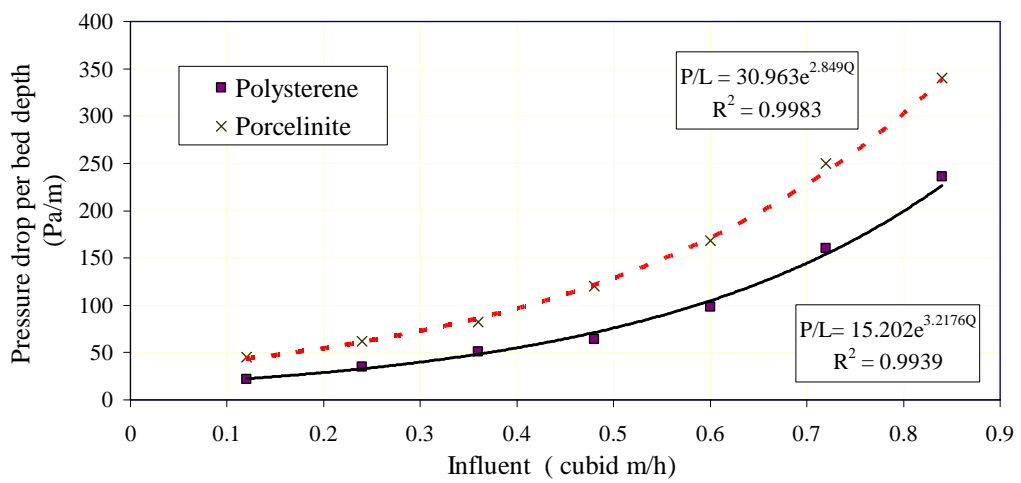


Figure (4) The Effect Of Influent On Pressure Drop Per Unit Bed Depth Of SABR For Different Clean Bed Materials

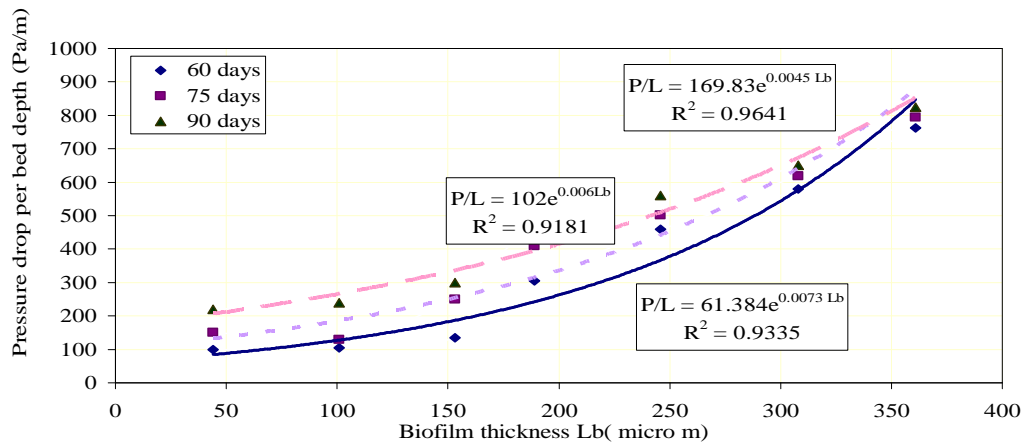


Figure (5) The Effect Of Biofilm Thickness On Pressure Drop Per Porcelinaite Bed Depth In SABR

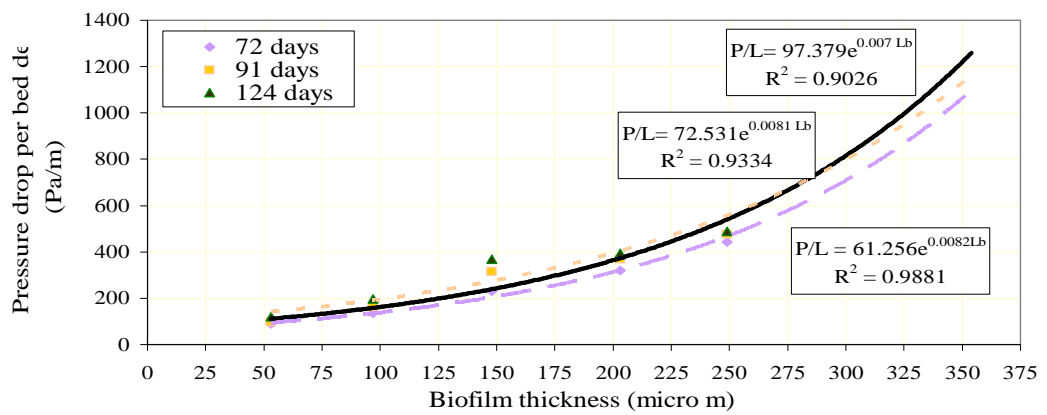


Figure (6) The Effect Of Biofilm Thickness On Pressure Drop Per Polysterne Bed Depth In SABR